








ORIGINAL RESEARCH

OPEN ACCESS



## TIGIT blockade enhances functionality of peritoneal NK cells with altered expression of DNAM-1/TIGIT/CD96 checkpoint molecules in ovarian cancer

Ralph Ja Maas , Janneke S Hoogstad-van Evert <sup>a,b,\*</sup>, Jolien Mr Van der Meer <sup>a,\*</sup>, Vera Mekers <sup>a</sup>, Somayeh Rezaeifard <sup>a</sup>, Alan J Korman <sup>c,d</sup>, Paul Kjd de Jonge <sup>a</sup>, Jeannette Cany<sup>a</sup>, Rob Woestenenk<sup>a</sup>, Nicolaas Pm Schaap <sup>e</sup>, Leon F Massuger<sup>b</sup>, Joop H Jansen <sup>a</sup>, Willemijn Hobo <sup>a</sup>, and Harry Dolstra <sup>a</sup>

<sup>a</sup>Department of Laboratory Medicine, Laboratory of Hematology, Radboud University Medical Center, Nijmegen, The Netherlands; <sup>b</sup>Department of Obstetrics and Gynecology, Radboud University Medical Center, Nijmegen, The Netherlands; <sup>c</sup>Bristol-Myers Squibb, Redwood City, CA, USA;; <sup>d</sup>AK Vir Biotechnology, San Francisco, CA, USA; <sup>e</sup>Department of Hematology, Radboud University Medical Center/Radboud Institute for Molecular Life Sciences, Nijmegen, The Netherlands

### ABSTRACT

Advanced ovarian cancer (OC) patients have a poor 5-year survival of only 28%, emphasizing the medical need for improved therapies. Adjuvant immunotherapy could be an attractive approach since OC is an immunogenic disease and the presence of tumor-infiltrating lymphocytes has shown to positively correlate with patient survival. Among these infiltrating lymphocytes are natural killer (NK) cells, key players involved in tumor targeting, initiated by signaling via activating and inhibitory receptors. Here, we investigated the role of the DNAM-1/TIGIT/CD96 axis in the anti-tumor response of NK cells toward OC. Ascites-derived NK cells from advanced OC patients showed lower expression of activating receptor DNAM-1 compared to healthy donor peripheral blood NK cells, while inhibitory receptor TIGIT and CD96 expression was equal or higher, respectively. This shift to a more inhibitory phenotype could also be induced *in vitro* by co-culturing healthy donor NK cells with OC tumor spheroids, and *in vivo* on intraperitoneally infused NK cells in SKOV-3 OC bearing NOD/SCID-IL2R $\gamma$  null (NSG) mice. Interestingly, TIGIT blockade enhanced degranulation and interferon gamma (IFN $\gamma$ ) production of healthy donor CD56<sup>dim</sup> NK cells in response to OC tumor cells, especially when DNAM-1/CD155 interactions were in place. Importantly, TIGIT blockade boosted functional responsiveness of CD56<sup>dim</sup> NK cells of OC patients with a baseline reactivity against SKOV-3 cells. Overall, our data show for the first time that checkpoint molecules TIGIT/DNAM-1/CD96 play an important role in NK cell responsiveness against OC, and provides rationale for incorporating TIGIT interference in NK cell-based immunotherapy in OC patients.

### ARTICLE HISTORY

Received 11 May 2020  
Revised 1 October 2020  
Accepted 25 October 2020

### KEYWORDS



Ovarian cancer; TIGIT; DNAM-1; CD96; NK cells; checkpoint blockade

## Introduction

Patients with ovarian carcinoma (OC) are mostly diagnosed at advanced stage, as many women do not show clear symptoms at an early stage. This late detection of advanced disease is associated with poor prognosis and poor quality of life.<sup>1</sup> Current therapy for OC is debulking surgery combined with chemotherapy, yet the 5-year survival for advanced OC is only 28%.<sup>2</sup> Adjuvant immunotherapy could be a complementary approach since OC is considered to be an immunogenic disease and the presence of tumor-infiltrating lymphocytes (TILs) positively correlates with survival.<sup>3</sup> Several reports showed that prolonged survival associated mainly with the presence of CD8<sup>+</sup> cytotoxic T cells,<sup>4,5</sup> yet it has also been described that CD103<sup>+</sup> tumor-infiltrating NK cells often co-infiltrate with CD8<sup>+</sup>CD103<sup>+</sup> T cells suggesting both T and NK cell involvement in anti-OC immune responses.<sup>6</sup> Recently, we observed that a higher NK cell percentage within the ascitic lymphocyte fraction was correlated with enhanced survival of OC patients.<sup>5</sup> Furthermore, multiple studies have demonstrated that OC cells


are susceptible to killing by activated NK cells.<sup>7–9</sup> Hence, increasing NK cell immunity in OC patients by immunotherapeutic strategies could be an attractive strategy. Boosting peritoneal NK cell responses with IL-15 receptor-mediated stimulation and intraperitoneal NK cell adoptive transfer are being explored as therapeutic approaches in OC.<sup>10–12</sup> However, intrinsic and adoptive NK cell antitumor immunity in OC patients can be attenuated by immunosuppressive cells and cytokines within the tumor microenvironment.<sup>13–16</sup> Identification of and interference with these immunosuppressive pathways may further improve the efficacy of NK cell-based immunotherapy.

NK cells are generally characterized according to their expression of CD56 and CD16 surface antigens in CD56<sup>dim</sup>CD16<sup>high</sup> and CD56<sup>bright</sup>CD16<sup>neg</sup> NK cells. According to the tissue type and the pathological conditions, the frequency and distribution of these NK cell populations may vary.<sup>17,18</sup> Furthermore, cytokines and other soluble factors present in ascitic fluid of OC patients can have a strong effect

**CONTACT** Harry Dolstra  [harry.dolstra@radboudumc.nl](mailto:harry.dolstra@radboudumc.nl)  Department of Laboratory Medicine - Laboratory of Hematology, Radboud University Nijmegen Medical Center, Nijmegen, The Netherlands

\*authors contributed equally

**Grants:** This work was supported by grants from RIMLS 2016-7

 Supplemental data for this article can be accessed on the [publisher's website](#).

© 2020 The Author(s). Published with license by Taylor & Francis Group, LLC.

This is an Open Access article distributed under the terms of the Creative Commons Attribution-NonCommercial License (<http://creativecommons.org/licenses/by-nc/4.0/>), which permits unrestricted non-commercial use, distribution, and reproduction in any medium, provided the original work is properly cited.

on the phenotype and distribution of different subsets of NK cells.<sup>19</sup> For instance, transforming growth factor (TGF)- $\beta$  exerts immune-suppressive action on NK cells and can partially convert healthy peripheral blood CD56<sup>dim</sup>CD16<sup>high</sup> NK cells to CD56<sup>bright</sup>CD16<sup>low/neg</sup>.<sup>19</sup> Functionally, NK cells are regulated by the net balance of signals perceived by their activating and inhibiting receptors which enables NK cells to effectively kill target cells that have increased expression of stress-induced ligands or lack sufficient inhibitory signals, while maintaining self-tolerance.<sup>18,19</sup> These NK cell receptors can be grouped in MHC class I-specific receptors versus non-MHC binding receptors. Important non-MHC binding activating receptors on NK cells are DNAX Accessory Molecule-1 (DNAM-1), NKG2D, and natural cytotoxicity receptors (NCRs), while inhibitory receptors including T cell immunoglobulin and ITIM domain (TIGIT) keep the NK cell response in check.<sup>20</sup> TIGIT shares its ligands CD155 (or poliovirus receptor/PVR) and CD112 (or Nectin-2) with DNAM-1. CD96 (or TACTILE) also binds CD155, but in human NK cell signaling its function remains elusive. CD155 and CD112 are mainly expressed by antigen-presenting cells (APCs), activated T cells, fibroblasts, and endothelial cells in healthy tissues.<sup>21,22</sup> Furthermore, CD112/CD155 are upregulated upon cellular stress and are therefore highly expressed on several types of cancer amongst which OC.<sup>23,24</sup> CD112 binds to DNAM-1 but only weakly to TIGIT, while CD155 has high affinity for both TIGIT and DNAM-1.<sup>25–27</sup> NK cell cytotoxicity is triggered by DNAM-1 crosslinking, resulting in Fyn-mediated phosphorylation of the cytoplasmic tyrosine residues.<sup>28</sup> TIGIT signaling is mediated via immunoreceptor tyrosine-based inhibitory (ITIM) and immunoglobulin tail tyrosine (ITT)-like motifs, through which inhibitory signals are conducted that impair cytotoxicity, granule polarization, and cytokine secretion in NK cells.<sup>29,30</sup> The DNAM-1/TIGIT/CD96 axis on NK cells was recently elaborately reviewed by Sanchez-Correa *et al.*<sup>31</sup>

DNAM-1 on NK cells is downregulated in most cancer types including OC, colon carcinoma, and acute myeloid leukemia (AML).<sup>32–35</sup> Carlsten *et al.* showed that DNAM-1 is an important activating NK cell receptor in OC and that CD155 expression on patient-derived OC tumor cells correlates with a reduction in DNAM-1 expression.<sup>34</sup> Similarly, reduced expression of DNAM-1 on NK cells from AML patients was observed, which was negatively correlated with CD112 expression on blasts.<sup>32</sup> Moreover, NK cells expressing high levels of TIGIT were associated with poor survival in AML patients.<sup>36</sup> These TIGIT<sup>high</sup> NK cells were found to be more susceptible to myeloid-derived suppressor cell (MDSC) inhibition compared to TIGIT<sup>low</sup> NK cells.<sup>37</sup> Furthermore, TIGIT could be upregulated through recombinant human (rh)IL-15 stimulation, which was associated with lower IFN $\gamma$  production.<sup>37,38</sup> These studies underscore the importance of TIGIT as an important inhibitory receptor on NK cells with clinical impact, reflected by the promising efficacy of TIGIT blockade on NK cell reactivity in colon and breast cancer.<sup>39,40</sup>

In this report, we investigated the role of TIGIT in the functional impairment of NK cells in OC patients. We demonstrated that NK cells from healthy donors, as well as OC patients, exhibit high expression of TIGIT, while DNAM-1 is

strongly reduced on ascites-derived NK cells from patients. Moreover, we showed that this DNAM-1 downregulation on NK cells is mediated by OC tumor cell exposure. Most importantly, we showed augmented tumor reactivity of NK cells from both healthy donors and OC patients following TIGIT blockade, thereby providing a rationale for incorporating TIGIT interference in NK cell-based immunotherapy in OC patients.

## Methods

### Patient samples

Malignant ascites fluid samples were collected after written informed consent at first surgery of patients with stage IIIc or IV high-grade serous papillary OC at the Radboud University Medical Center (Radboudumc). Study approval was given by the Regional Committee for Medical Research Ethics (CMO 2018–4845) and performed according to the Code for Proper Secondary Use of Human Tissue (Dutch Federation of Biomedical Scientific Societies, [www.federa.org](http://www.federa.org)). The progression-free survival (PFS) and overall survival (OS) at time of analysis, CA-125 levels, and treatment status are shown for individual patients in Table 1. Ascites was filtered using a 100  $\mu$ m filter, centrifuged, and cells were resuspended in phosphate-buffered saline (PBS). Subsequently, mononuclear cells were isolated using a Ficoll-Hypaque (1.077 g/mL; GE Healthcare, 17–1440–03) density gradient. For the benign controls, samples were collected at benign gynecological surgeries. The main indication for diagnostic laparoscopy was abdominal pain and samples were included only if pathological findings were absent. Detection of cysts, endometriosis, and adhesions at laparoscopy was exclusion criteria. All samples were cryopreserved in dimethyl sulfoxide (DMSO)-containing medium and used after thawing.

### NK cell isolations

Peripheral blood mononuclear cells (PBMCs) were obtained from healthy donor buffy coats (Sanquin Blood Bank, Nijmegen, the Netherlands) by density gradient Ficoll-Hypaque centrifugation. NK cells were isolated from PBMCs of healthy donors or cryopreserved ascites-derived mononuclear cells using a magnetic bead-based NK cell enrichment kit (StemCell Technologies, #19055) according to manufacturer's instructions. Further purification of ascites-derived NK cells was performed via fluorescence-activated cell sorting (FACS) based on lymphocyte sized forward/side scatter using the FACS Aria (BD Bioscience) to eliminate any remaining tumor cells. All isolations resulted in  $\geq 90\%$  purity.

### Cell culture

The OC cell lines SKOV-3 (RRID:CVCL\_0532) and IGROV-1 (RRID:CVCL\_1304) were cultured in Roswell Park Memorial Institute medium 1640 (RPMI; Gibco, #11875091) supplemented with 10% fetal calf serum (FCS; Integro), and OVCAR-3 (RRID:CVCL\_0465) was cultured with RPMI supplemented with 20% FCS and 1  $\mu$ g/mL bovine albumin (Sigma, #I0516). K562 (RRID:CVCL\_0004) was cultured in Iscove's Modified

**Table 1.** Ovarian cancer patient characteristics and DNAM-1/TIGIT expression profile.

Patient Characteristics			CD56dim NK cell population												
Patient no.	EOC Stage	CA125 (U/mL)	Treatment	Complete	PFS (months)	OS (months)	DNAM-1 gated (%)	DNAM-1 (ΔMFI)	TIGIT gated (%)	TIGIT (ΔMFI)	Responder (≥10% CD107a)	CD107a Control	CD107a TIGIT blockade	IFNy control	IFNy TIGIT blockade
1	3 c	1304	Interval debulking	Complete	8.4	29.4	NA	NA	NA	NA	Yes	14	22	4	7
2	4	1800	Interval debulking	Complete	0	8.6	79	0.90	38	1.8	Yes	10	21	3	8
3	3 c	358	Primary debulking	Optimal	0	28.8	46	0.40	48	2.7	Yes	26	34	8	9
4	3 c	1242	Primary debulking	Optimal	0	13.7	43	0.30	33	1	No	4	5	1	2
5	4	1400	chemotherapy	Treatment not continued	0	1.7	55	0.40	37	2.6	No	3	5	1	0
6	3 c	2380	Primary debulking	Optimal	20.5	55.5	15	0.10	78	4.8	Yes	22	27	3	4
7	3 c	928	Interval debulking	Complete	23.9	41.3	23	0.30	69	4.8	No	1	1	0	0
8	4	1223	Interval debulking	Optimal	4.1	9.4	81	1.17	29	1.79	Yes	37	51	34	46
9	4	1430	Interval debulking	Optimal	12.2	54.6	59	0.64	16	0.88	Yes	38	51	27	35
10	3 c	2528	Primary debulking	Complete	17.2	54	61	0.60	34	1.3	NA	NA	NA	NA	NA

Characteristics of ovarian cancer patients from whom NK cells were phenotyped and functionally assessed. Patient samples were obtained at diagnosis. EOC, Epithelial Ovarian Cancer; PFS, Progression-Free Survival; OS, Overall Survival; MFI, Median Fluorescence Intensity; NA, not applicable.

Dulbecco's medium (IMDM; Gibco, #12440061) containing 10% FCS. Cell lines were tested for mycoplasma contamination with MycoAlert™ Mycoplasma Detection Kit (Lonza, #LT07-418) every 6 months. All cell lines were cultured for a maximum of 3 months. SKOV-3 and K562 were purchased from the ATCC. IGROV-1 and OVCAR-3 were a kind gift from Prof. Dr. OC Boerman, Department of Nuclear Medicine, Radboud University Medical Center, Nijmegen, the Netherlands. Primary low-grade serous OC cell line ASC009 was generated by NTRC in Oss, the Netherlands, from primary ascites material and a kind gift from Guido Zaman.

### **Multicellular tumor spheroids**

OC tumor spheroids were generated by seeding  $3 \times 10^4$  (SKOV-3),  $6 \times 10^4$  (IGROV-1), and  $12 \times 10^4$  (OVCAR-3) cells/well in a volume of 100  $\mu$ L/well of culture medium in 96-well plates pre-coated with 1% agarose in Dulbecco's Modified Eagle Medium/Nutrient Mixture F-12 medium (DMEM/F12; Invitrogen 11330-057, adjusted from Giannattasio et al. and Friedrich et al.<sup>41,42</sup> Tumor spheroids were used for functional assays upon reaching a solid state at 4 days after initial seeding. For phenotypical analysis, 26,000 NK cells were seeded with concentrations of rhIL-15 ranging from 0.01 to 10 nM (Immunotools) and re-treated with the same rhIL-15 dose on day 3. After 7 days, spheres were harvested, trypsinized with TrypLE™ Express (ThermoFisher, #12605028) for 45 minutes, washed, and analyzed.

### **Ovarian cancer tissue**

Tissue was transferred to DMEM/F12 medium (Invitrogen 11330-057) supplemented with 10% FCS and 1% Penicillin-Streptomycin at 4°C. The next day, the tissue was mechanically minced using a scalpel and filtered through a 70  $\mu$ m cell strainer to obtain a single-cell suspension. For phenotypical analysis, 50,000–100,000 NK cells and the same number of OC tissue cells were seeded with concentrations of rhIL-15 (Immunotools, 11340158) ranging from 0.01 to 10 nM and re-supplemented with the same rhIL-15 dose on day 4. After 7 days, suspension cells were harvested, washed, and analyzed.

### **Flow cytometry (FCM)**

For phenotypical analysis, cells were incubated with antibodies in FCM buffer (PBS/0.5% bovine serum albumin) for 20 min at 4°C. After washing, cells were resuspended in FCM buffer and analyzed on a Gallios flow cytometer (Beckman Coulter). The following fluorochrome-conjugated monoclonal antibodies and life/dead stains were used: DNAM-1-FITC (clone DX11, BD Bioscience, #559788), TIGIT-APC (clone 741182, R&D systems, #FAB7898A), CD96-BV421 (clone NK92.39, Biolegend, #338418), CD96-PE-Dazzle (clone NK92.39, Biolegend, #338414) CD19-FITC (clone HD37, DAKO, #F0768), CD3-ECD (clone UCHT1, Beckman Coulter, #A07748), CD14-PE-Cy7 (clone HCD14, Biolegend, #325618), CD56-BV510 (clone HCD56, Biolegend, #318340), CD45-AF700 (clone HI30, Biolegend, #304024), KLRG-1 FITC (clone REA261, Miltenyi Biotec, #130-103-640), LIGHT PE

(clone 7-3(7), eBioscience, #12-2589-42), CD160 PE-Cy7 (clone BY55, Biolegend, #341211), 4-1BB APC (clone 4B4-1, BD Bioscience, #220890), CD57 BV421 (clone NK-1, BD Bioscience, #563896), SIGLEC-9 FITC (clone REA492, Miltenyi Biotec, #130-107-607), SIGLEC-7 APC (clone 6-434, Biolegend, #339206), NKG2C PE (clone 134591.0, R&D Systems, #FAB138P), NKG2D PE-Cy7 (clone 1D11, Biolegend, 320812), NKp46 BV421 (clone 9E2, Biolegend, #331914), NKG2a APC (clone Z199, Beckman Coulter, #A60797), PD-1 BV421 (clone EH12.1, BD Bioscience, #562516), BTLA PE (clone J168-540, BD Bioscience, #558485), OX-40 PE-Cy7 (clone Ber-ACT35, Biolegend, #350011), 2B4 FITC (clone C1.7, Biolegend, #329506), CD112 PE-Cy7 (clone TX31, Biolegend, #337414), CD155 BV421 (clone SKII.4, Biolegend, 337631), fixable viability dye eFluor780 (eBiosciences, #65-0865-14) and 7-AAD (Sigma, #A9400-1 MG). All flow cytometric data were analyzed with Kaluza 2.1 software from Beckman Coulter.

### **NK cell activity assay**

Isolated NK cells were plated in a flat bottom 96 wells plate (Corning Star) at 100,000 cells/well and cultured overnight in IMDM supplemented with 10% FCS in the presence of 1 nM rhIL-15 (Immunotools, 11340158). The next day, NK cells were co-cultured with OC cell lines SKOV-3, IGROV-1, OVCAR-3 or K562 target cells (100,000 cells per well for all cell lines) in the presence of 10  $\mu$ g/ml anti-TIGIT hIgG1.3 FC silenced blocking antibody (Bristol-Myers Squibb), hIgG 1.3 FC silenced isotype control (Bristol-Myers Squibb), anti-DNAM-1 (clone 11A8, Biolegend, #338302), anti-CD96 (clone NK92.39, Biolegend, #338402) or hIgG1 (clone MOPC, BioXcell, BE0083). In addition, CD107a-PECy7 (clone H4A3, Biolegend, #328618) and Brefeldin A (BD, #555029) were added to the culture. All conditions were performed in triplicate. After 4 h, cells were harvested and washed with PBS. After subsequent staining for CD56-APC (clone HCD56, Biolegend, #318310), CD45-AF700 and eFluor780 for 20 minutes at 4°C, cells were intracellularly stained for IFN $\gamma$ -FITC (clone B27, BD Bioscience, #554700) with fixation/permeabilization buffer (eBioscience, #00-5123-43, #005223-56 and #00-8333-56) according to manufacturer's instructions. Cells were analyzed on the Gallios flow cytometer.

### **In vivo SKOV-3 NK cell phenotype tumor model**

All *in vivo* experiments were approved by the Radboudumc animal care and user committee (DEC 2015-123). Ten 6–20 weeks old female NOD/SCID/IL2R $\gamma$ null (NSG) mice (Jackson laboratories), with an average weight of 25 g, were divided randomly into two groups. One group received an intraperitoneal (i.p.) infusion with  $1.0 \times 10^6$  SKOV-3-GFP-Luc cells and the control group received a PBS injection. Bioluminescence imaging (BLI) was performed weekly until saturation. For this, mice were injected i.p. with 150 mg/kg D-luciferin (PerkinElmer 122796), anesthetized with isoflurane and after 10 min bioluminescence images were collected in an IVIS using the Living Image processing software. Regions of Interest (ROIs) were drawn around the abdominal area, and



measurements were automatically generated as integrated flux of photons (photons/s). After 49 days, all mice received i.p. peripheral blood NK cell infusion ( $3.8 \times 10^6$  cells/mouse) derived from a healthy donor. In addition, all mice received i.p. recombinant human rhIL-15 (2.5  $\mu$ g/mouse, Immunotools, 11340158) every 2 days. Fourteen days after NK cell infusion, mice were sacrificed and an abdominal lavage was performed with 8 mL PBS. NK cells from this lavage were used for NK cell activity assays and phenotyping.

### ***In vivo* SKOV-3 NK cell plus TIGIT blockade tumor model**

Forty-five 6–20 weeks old female NOD/SCID/IL2R $\gamma$  null (NSG) mice (Jackson laboratories), with an average weight of 24 g, were divided randomly into three groups. All groups received an intraperitoneal (i.p.) infusion with  $0.2 \times 10^6$  SKOV-3-GFP-Luc cells. BLI imaging was performed weekly as described above. After 4 days, two groups received an i.p. peripheral blood NK cell infusion ( $5.4 \times 10^6$  cells/mouse) derived from a healthy donor. In addition, all mice received i.p. recombinant human rhIL-15 (2.5  $\mu$ g/mouse, Immunotools, 11340158) every 2 days and weekly injections of nanogram. Mice receiving NK cells were also injected twice weekly with either isotype control B12-LALAPG Fc silenced antibodies (custom ordered, Evitrea) or anti-TIGIT hIgG1.3 Fc silenced blocking antibodies (Bristol-Myers Squibb). Control mice not receiving NK cells were also treated with isotype control B12-LALAPG Fc silenced antibodies. Thirty-three days after SKOV-3 tumor cell infusion, mice were sacrificed and an abdominal lavage was performed as described above. Harvested cells were quantified using Flow-Count Fluorospheres (Beckman Coulter, 7547053) according to manufacturer's instructions. NK cells from this lavage were used for an NK cell activity assay.

**Statistics** Data analysis was conducted by Prism software (GraphPad, version 5.03 for Windows) and SPICE software (version 5). For normally distributed data the Student t-test (paired or unpaired) or One-way ANOVA (with or without repeated measure) was used where applicable as stated in the figure legends. Non-normally distributed data were tested with a Wilcoxon signed-rank test, Mann-Whitney test, Kruskal-Wallis or Friedman test where applicable as stated in the figure legends. For statistical comparison of SPICE pie charts, the built-in test in SPICE software was used, applying 1,000,000 permutations. A *p*-value of <0.05 was considered statistically significant.

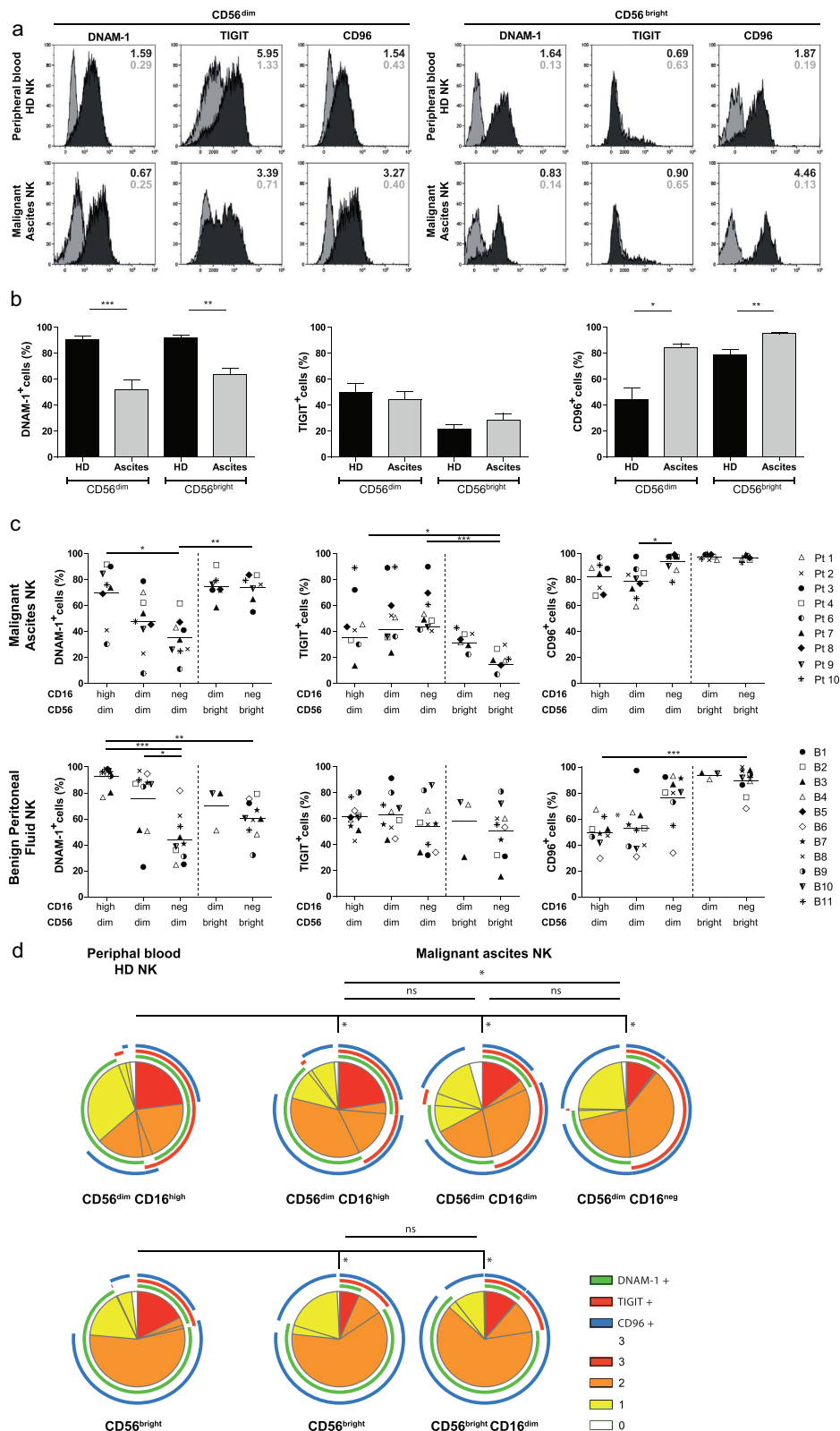
## **Results**

### ***Peritoneal NK cells of OC patients consist of multiple distinct CD56<sup>dim</sup> subpopulations which have reduced DNAM-1 expression***

Flow cytometric analysis was performed on peritoneal NK cells from OC patients, peritoneal NK cells from patients with benign conditions, and peripheral blood NK cells from healthy donors to determine the DNAM-1, TIGIT, and CD96 expression levels on CD56 positive NK cell subsets. For this, we analyzed CD56<sup>dim</sup> and CD56<sup>bright</sup> NK cells derived from ascites

of high-grade serous OC patients (N = 9) and compared them to healthy donors (N = 10, **Figures 1a-c**). CD56<sup>dim</sup> and CD56<sup>bright</sup> NK cells were defined as shown in Supplemental fig S1A-E for malignant ascites of patients, healthy donor peripheral blood and benign peritoneal fluid. We confirmed that DNAM-1 expression was significantly reduced in both peritoneal CD56<sup>dim</sup> and CD56<sup>bright</sup> NK cells from OC patients ( $51.8\% \pm 23.4\%$  and  $64.1\% \pm 13.6\%$ , respectively; **Figure 1b**) compared to healthy donor NK subsets ( $90.9\% \pm 7.7\%$  and  $91.8\% \pm 7.4\%$ , respectively; **Figure 1b**). Notably, TIGIT expression was similar for ascites-derived NK cells and healthy donor NK cells, with higher expression on CD56<sup>dim</sup> compared to CD56<sup>bright</sup> NK cells **Figure 1b**. Expression of CD96 was significantly higher in both CD56<sup>dim</sup> and CD56<sup>bright</sup> NK cell subsets in ascites ( $84.2\% \pm 9.3\%$  and  $95.1\% \pm 3.0\%$ , respectively; **Figure 1b**) compared to healthy donor NK cells ( $44.1\% \pm 28.2\%$  and  $78.8\% \pm 13.6\%$ , respectively; **Figure 1b**). In a separate experiment, we also assessed the phenotype of peritoneal fluid NK cells of benign patients and found intermediate DNAM-1 positivity in CD56<sup>dim</sup> and CD56<sup>bright</sup> NK cells ( $69.7\% \pm 25.8\%$  and  $62.4\% \pm 11.7\%$ , respectively) as shown in Supplemental fig S1F. CD96, similarly to DNAM-1 was moderately positive in CD56<sup>dim</sup> and CD56<sup>bright</sup> NK cells in benign peritoneal fluid ( $50.7\% \pm 26.6\%$  and  $90.1\% \pm 8.7\%$ , respectively). Unfortunately, TIGIT expression of benign patients could not be compared directly because of a different fluorescence intensity of the antibody used in the two different studies. These data reveal that the balance shifts toward higher expression of inhibitory receptor CD96 while activating receptor DNAM-1 is reduced on peritoneal NK cells of OC patients.

As expected in healthy donors we observed a clear distinction between CD56<sup>dim</sup> CD16<sup>high</sup> and CD56<sup>bright</sup> CD16<sup>neg</sup> NK cell subsets, but for peritoneal-derived NK cells, we found altered CD56 and CD16 expression patterns (Supplemental fig S1E). Based on a minimum of 100 events, three distinct populations of CD56<sup>dim</sup> NK cells were defined; i.e. CD56<sup>dim</sup> CD16<sup>high</sup>, CD56<sup>dim</sup> CD16<sup>low</sup> and CD56<sup>dim</sup> CD16<sup>neg</sup> NK cells, each having different expression patterns of DNAM-1, TIGIT and CD96 (**Figure 1c**, Supplemental fig S1G). In addition, we found the CD56<sup>bright</sup> CD16<sup>neg</sup> NK cell subset besides a small CD56<sup>bright</sup> population with low CD16 expression in some donors, which exhibit similar expression levels of DNAM-1, TIGIT, and CD96. The conventional CD56<sup>dim</sup> CD16<sup>high</sup> NK cells seemed similar in OC patients and healthy donors, but with slightly lower DNAM-1 expression and higher CD96 expression in OC. Interestingly, within the three ascites-derived CD56<sup>dim</sup> populations, DNAM-1 expression gradually decreased in parallel with decreasing CD16 expression **Figure 1c**. In contrast, CD96 expression significantly increased with loss of CD16 expression, while TIGIT expression remained unaltered and is exclusively expressed by the CD56<sup>dim</sup> populations in malignant ascites. CD56<sup>dim</sup> CD16<sup>high</sup> NK cells from benign patients resemble healthy donor peripheral blood NK cells with a high percent of DNAM-1 and low percent CD96 relative to malignant ascites-derived NK cells. However, CD56<sup>dim</sup> CD16<sup>low</sup> NK cells from benign peritoneal fluid have an equally low percent DNAM-1 and increased percent CD96 as observed in OC patients **Figure 1c**. To look at these co-expression profiles from a different angle, we performed SPICE analysis. This analysis demonstrated that healthy donor



CD56<sup>dim</sup> NK cells had significantly different co-expression patterns of DNAM-1, TIGIT, and CD96 compared to the three ascites-derived CD56<sup>dim</sup> NK cell subsets as healthy donor NK cells expressed more DNAM-1 and less CD96 **Figure 1d**. Within the three different OC subsets, the CD56<sup>dim</sup> CD16<sup>high</sup> NK cells were significantly different from CD56<sup>dim</sup> CD16<sup>neg</sup> NK cells but not CD56<sup>dim</sup> CD16<sup>low</sup> NK cells which is mainly attributed by DNAM-1 expression which is high on CD56<sup>dim</sup> CD16<sup>high</sup>, intermediate on CD56<sup>dim</sup> CD16<sup>low</sup> and lowest on CD56<sup>dim</sup> CD16<sup>neg</sup> NK cells. As a result, CD56<sup>dim</sup> CD16<sup>neg</sup> OC derived NK cells showed an enlarged population with TIGIT/CD96 co-expression whereas the majority of CD16<sup>+</sup> NK cells had more CD96/DNAM-1 co-expression indicating that CD56<sup>dim</sup> CD16<sup>neg</sup> have a more inhibitory phenotype and CD56<sup>dim</sup> CD16<sup>high</sup> a more activatory phenotype these populations have a more inhibitory and activating phenotype, respectively.

Collectively, these data demonstrate that peritoneal NK cells in OC patients display an altered expression pattern of the DNAM-1/TIGIT/CD96 axis compared to healthy donor NK cells that is indicative of a more inhibitory or exhausted phenotype.

### Expression of DNAM-1/TIGIT/CD96 axis members on NK cells is increased upon rhIL-15 stimulation and shifts to a more inhibitory phenotype upon engagement with OC tumor cells

To further investigate the effect of OC cells on DNAM-1/TIGIT/CD96 expression levels by NK cells, we co-cultured healthy donor NK cells for one week with OC spheroids, generated from the cell lines SKOV-3, IGROV-1, and OVCAR-3, in the presence of increasing rhIL-15 concentrations to support NK cell survival. DNAM-1, TIGIT, and CD96 expression levels were all upregulated on CD56<sup>dim</sup> NK cells by rhIL-15, in a dose-dependent manner **Figure 2a**. Stimulation with either of the OC spheroids resulted in a strong decrease of DNAM-1 expression **Figure 2a**. In contrast, TIGIT and CD96 expression were not significantly affected by SKOV-3, IGROV-1, or OVCAR-3 spheroids at lower rhIL-15 concentrations. However, with higher levels of rhIL-15, also a trend in reduced CD96 and TIGIT expression was observed in the presence of SKOV-3 and/or IGROV-1 spheroids. In a similar 2D model with primary ascites-derived cell line ASC009, we found comparable results **Figure 2b**.

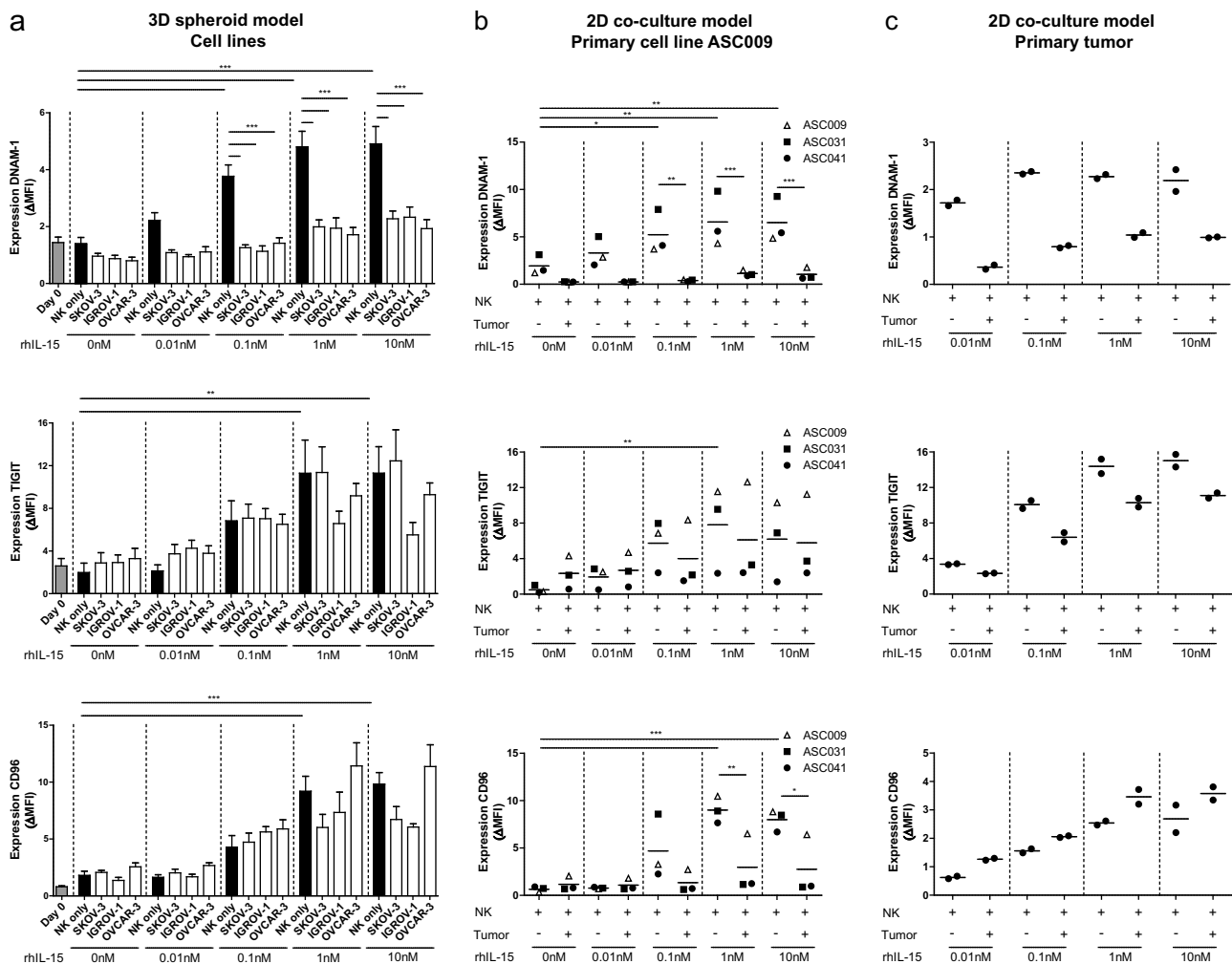


**Figure 2. DNAM-1, TIGIT and CD96 are dose-dependently upregulated by rhIL-15 and DNAM-1 is downregulated by OC tumor cells.** (a) DNAM-1 (n = 8), TIGIT (n = 6) and CD96 (n = 5) expression on NK cells of healthy donors co-cultured with SKOV-3, IGROV-1 or OVCAR-3 spheroids and increasing rhIL-15 concentrations for 7 days. Data is shown as mean±SEM. One-Way ANOVA with Bonferroni correction was used for statistical analysis, \*p < .05, \*\*p < .01 and \*\*\*p < .001. (b) DNAM-1, TIGIT and CD96 expression on healthy donor NK cells co-cultured with a patient-derived primary tumor cell line and increasing rhIL-15 concentrations for 7 days cultured in duplicate. (c) DNAM-1, TIGIT and CD96 expression on healthy donor NK cells co-cultured with patient-derived tumor cells and increasing rhIL-15 concentrations for 7 days cultured in duplicate.

To validate these results with primary high-grade OC material from a patient, we made a cell suspension of a small piece of tumor tissue and performed a co-culture with healthy donor NK cells for one week in the presence of rhIL-15. Indeed, we found that DNAM-1 was strongly reduced in the presence of primary tumor cells **Figure 2c**. Also, TIGIT expression was somewhat decreased, but CD96 was not affected. In addition to DNAM-1, TIGIT, and CD96, we also looked at other NK cell checkpoint molecules but found no significant differences between NK cells cultured with or without spheroids (Supplemental fig S2A). There was a trend toward lower NKG2D expression, but this was not significant. We also visualized these expression patterns in SPICE and again no differences between NK cells cultured with or without spheroids were seen.

Next, we investigated whether engagement of NK cells with OC tumors *in vivo* also alters DNAM-1/TIGIT/CD96 expression levels. For this, SKOV-3 tumor-bearing NSG mice were infused intraperitoneally with healthy donor NK cells **Figures 3a and b**. rhIL-15 was given every other day to support NK cell persistence, and after 14 days NK cells were harvested by peritoneal lavage. Flow cytometry analysis showed that NK cells from SKOV-3 bearing mice had significant lower DNAM-1 expression on both CD56<sup>dim</sup> and CD56<sup>bright</sup> NK cells compared to NK cells from non-tumor bearing control mice **Figures 3c-D**. TIGIT expression of CD56<sup>dim</sup> NK cells was not affected by *in vivo* exposure to SKOV-3 tumors. Similarly to the *in vitro* OC spheroid model, rhIL-15 had a potent stimulatory effect on TIGIT expression as the  $\Delta$ MFI (delta Median Fluorescence Intensity) was strongly increased at day 14 compared to day 0. DNAM-1 and CD96 levels were similar on the day of infusion and harvesting. To determine the functional implication of TIGIT expression *in vivo* on non-exposed and OC-exposed NK cells, we analyzed their reactivity at the single-cell level upon *ex vivo* re-stimulation with SKOV-3 cells in the absence and presence of TIGIT blocking antibody **Figures 3e-F**. Interestingly, TIGIT blockade increased degranulation and IFN $\gamma$  production activity of NK cells harvested from either SKOV-3 tumor-bearing mice or control mice **Figures 3e-F**. To assess, the importance of other checkpoint molecules besides DNAM-1 and TIGIT, we assessed expression levels of 4-1BB, CD57, 2B4, NKG2D, NKp46, LIGHT, CD160, BTLA, OX-40, PD-1, NKG2a, SIGLEC-7, SIGLEC-9, and KLRG-1: only KLRG-1 showed a decrease in the presence of tumor (Supplemental fig S2B).

Altogether, these data indicate that DNAM-1 and TIGIT are both upregulated by NK cells in response to rhIL-15 in a dose-dependent manner, while DNAM-1 expression is strongly decreased following exposure to OC cell line spheroids or patient-derived tumor cells.

### **TIGIT blockade effectively enhances degranulation and IFN $\gamma$ production by OC-reactive CD56<sup>dim</sup> NK cells**

We next analyzed the effects of TIGIT versus DNAM-1 blockade on NK cell responses against OC in more detail. First, we addressed this for healthy donor NK cells, as these cells appear more functional based on their phenotype and have higher DNAM-1 compared to ascites-derived NK cells **Figure 1**. Hereto, mononuclear cells (MNCs) or CD56-enriched cells (by negative selection) were rested overnight with low dose (1 nM) rhIL-15.

This revealed that DNAM-1 is somewhat upregulated on CD56<sup>dim</sup> NK cells in the isolated fraction, while TIGIT was significantly enhanced only in CD56<sup>dim</sup> NK cells in the non-selected MNC situation (Supplemental fig S3A-B). Notably, CD96 was upregulated on both CD56<sup>dim</sup> and CD56<sup>bright</sup> NK cells in all tested conditions. Interestingly, malignant ascites-derived NK cells showed similar expression patterns as healthy donor NK cells (Supplemental fig S4A-C). As overnight resting of enriched NK cells in the presence of rhIL-15 did not affect TIGIT expression, we continued with 1 nM rhIL-15 for subsequent TIGIT blocking studies using the three different OC cell lines as targets. Unstimulated NK cells and rhIL-15 stimulated NK cells showed little to no degranulation and IFN $\gamma$  production, whereas NK cells stimulated with K562 and rhIL-15 showed a strong response in both degranulation and IFN $\gamma$  (Supplemental fig S5A). Fold change of CD107a and IFN $\gamma$  response was calculated compared to tumor cell stimulation in the presence of rhIL-15. TIGIT blockade resulted in a 36% ( $\pm$  16%) increase in degranulation and 31% ( $\pm$  14%) increase in IFN $\gamma$  production against SKOV-3 by healthy donor CD56<sup>dim</sup> NK cells **Figure 4a**. In contrast, CD56<sup>bright</sup> NK cells did not respond to TIGIT blockade as these cells lack TIGIT expression (Supplemental fig S5B). As expected, DNAM-1 blockade effectively inhibited the degranulation and IFN $\gamma$  response of CD56<sup>dim</sup> **Figure 4a** and CD56<sup>bright</sup> (Supplemental fig S4A-B) NK cells toward SKOV-3. Simultaneous TIGIT and DNAM-1 co-blockade still impaired degranulation and IFN $\gamma$  production by healthy donor NK cells, indicating that DNAM-1 triggering is more dominant in regulating OC-reactivity of NK cells (Supplemental fig S5C). Notably, single CD96 blockade, or co-blockade of CD96 with TIGIT or DNAM-1 did not affect NK cell functionality. Similar results were found with the OC cell lines IGROV-1 and OVCAR-3 (**Figure 4b** and Supplemental fig S5D).

We observed that TIGIT blockade was most effective in improving NK cell reactivity against SKOV-3 and IGROV-1, but less prominent for the OVCAR-3 cell line. This correlated with CD155 expression but not CD112, as CD155 was absent on OVCAR-3 in contrast to high levels observed on both SKOV-3 and IGROV-1, while all three cell lines had medium to high expression of CD112 **Table 2**. To elucidate which TIGIT/DNAM-1 ligand, CD112, or CD155, is most dominant in NK cell reactivity against OC tumor cells, siRNA-treated SKOV-3 cells were used with substantially reduced CD112 or CD155 expression (Supplemental fig S6A). Decreased siRNA-mediated CD155 expression significantly lowered NK cell reactivity against SKOV-3 cells, whereas CD112 knockdown did not have a clear effect (Supplemental fig S6B-C).

Together, these data demonstrate that TIGIT blockade enhances degranulation and IFN $\gamma$  production of healthy donor CD56<sup>dim</sup> NK cells in response to OC tumor cells, especially when appropriate DNAM-1/CD155 interactions are in place.

### **CD56<sup>dim</sup> NK cell functionality can be elevated by TIGIT blockade in an *in vivo* mouse model and in a subset of OC patients**

Having demonstrated that healthy donor NK cell reactivity against OC tumor cells can be boosted by TIGIT blockade, we next investigated whether this effect was also apparent in more clinically relevant models. For this, SKOV-3 tumor-



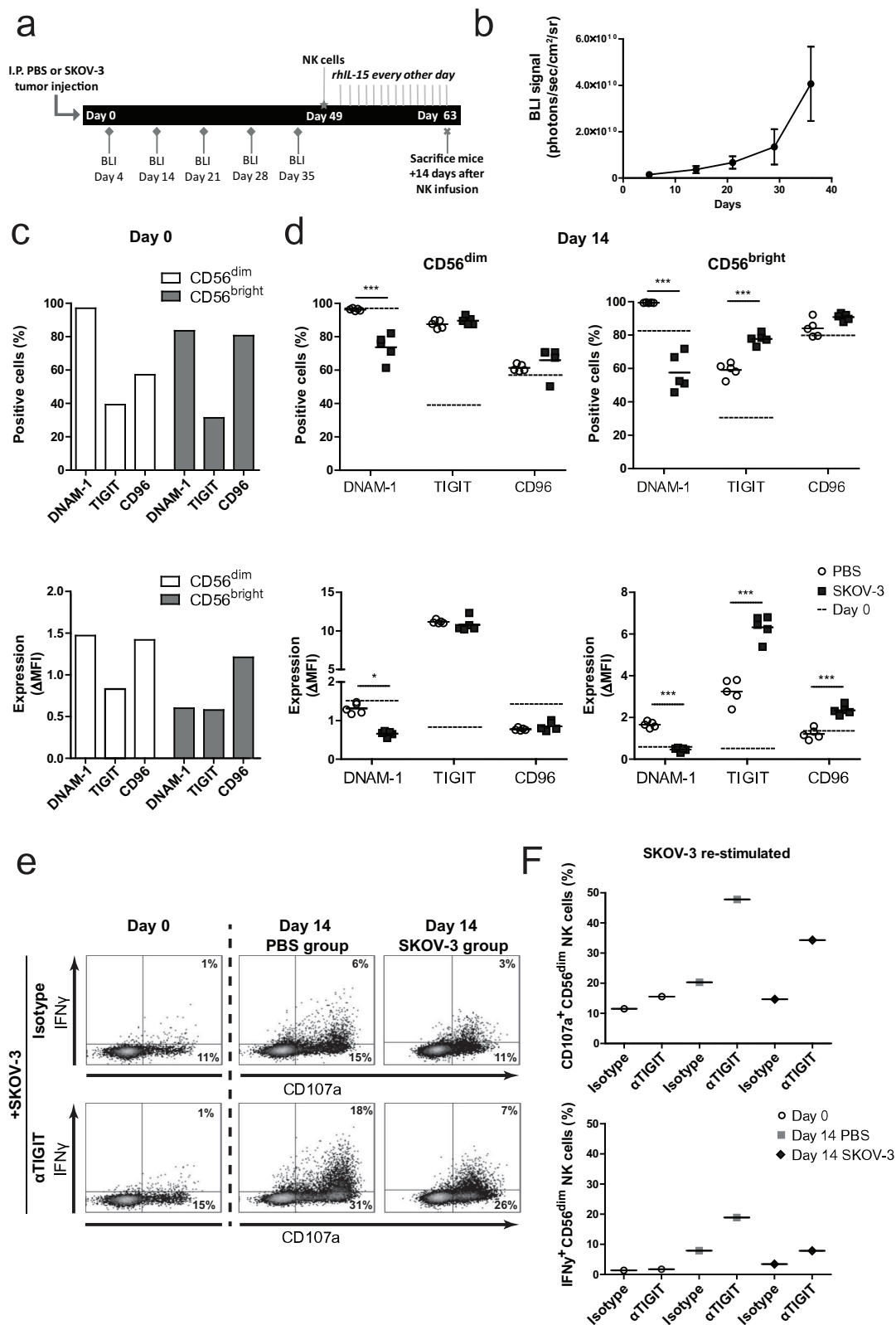


**Figure 3. SKOV-3 tumor-bearing mice have significantly reduced DNAM-1 expression in CD56<sup>dim</sup> and CD56<sup>bright</sup> NK cells.** (a) Schematic overview of the mouse experiment. (b) Bioluminescence imaging (BLI) signal of the SKOV-3 tumor-bearing mice over time ( $n = 5$ ). (c) Expression of DNAM-1, TIGIT and CD96 on CD56<sup>dim</sup> (left) and CD56<sup>bright</sup> (right) NK cells by flow cytometric measurement on day 0. The top graphs depict percentage positive cells and the bottom graphs depict  $\Delta$ MFI. (d) Expression of DNAM-1, TIGIT and CD96 on intraperitoneal NK cells harvested 14 days after adoptive transfer in SKOV-3 tumor-bearing NSG mice and control mice. Day 0 data is represented by dotted lines as a reference. The top graphs depict percentage positive cells and the bottom graphs depict  $\Delta$ MFI. Cumulative data are shown (lines indicate mean,  $n = 5$  per group). A One-Way ANOVA with Bonferroni correction was used for statistical analysis,  $* p < .05$  and  $*** p < .001$ . (e) Representative plots are shown of CD107a and IFN $\gamma$  expression by CD56<sup>dim</sup> NK cells after 4 h co-culture with SKOV-3 target cells, low dose rhIL-15 and TIGIT blockade or matching isotype control. (f) The percentage of CD107a and IFN $\gamma$  expressing CD56<sup>dim</sup> NK cells are shown on day 0 and day 14. Day 14 results are pooled NK cells from 5 different mice from either tumor-bearing or control mice.

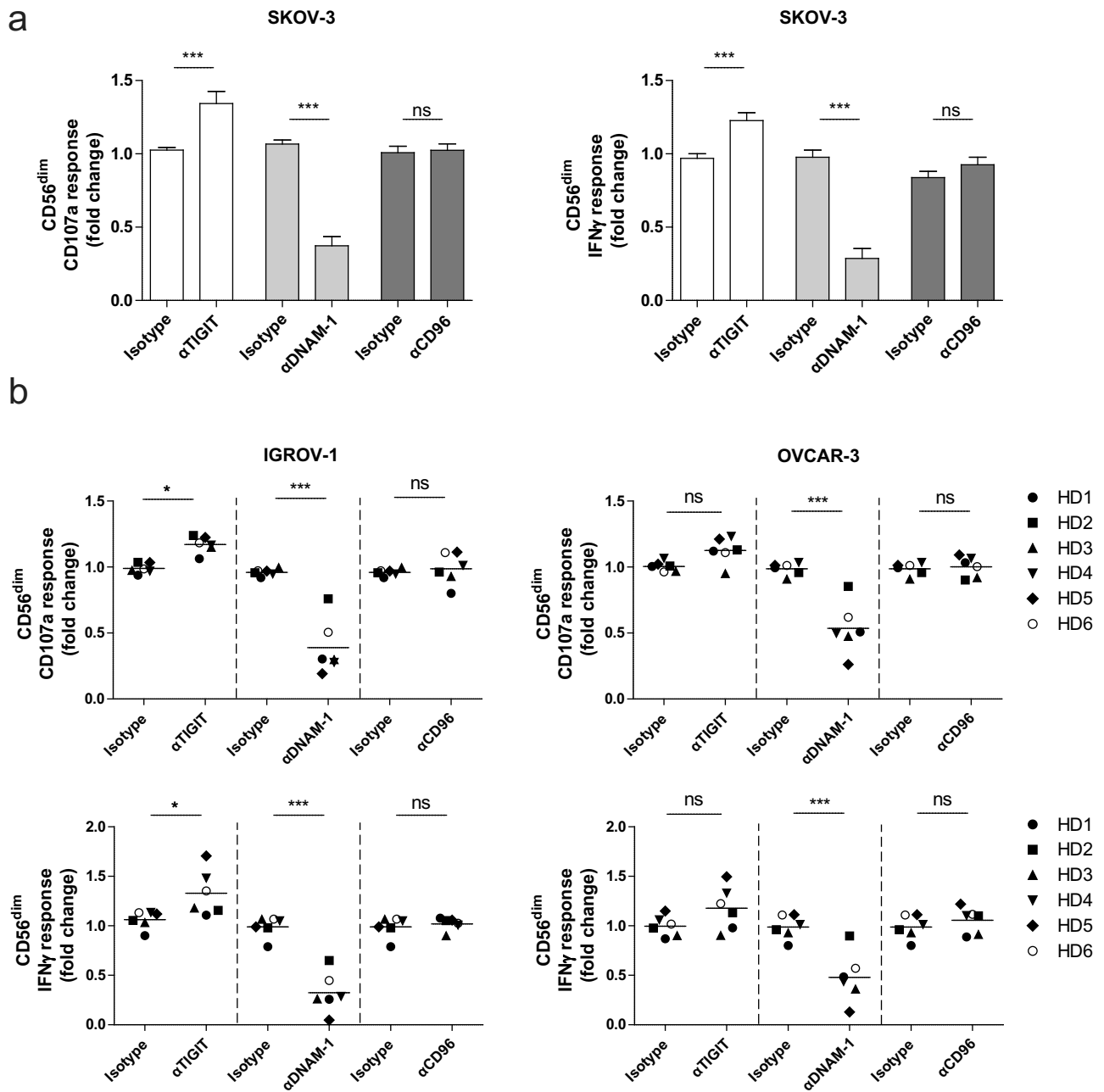


**Figure 4.** CD56<sup>dim</sup> NK cell degranulation toward OC cell lines is boosted by TIGIT blockade and inhibited by DNAM-1 blockade. (a) Healthy donor CD56<sup>dim</sup> NK cells fold change for CD107a and IFN $\gamma$  after 4 h stimulation with SKOV-3 target cells, low dose rhIL-15, and TIGIT, DNAM-1 and/or CD96 blockade or matching isotype controls. Fold change in CD107a and IFN $\gamma$  expression on CD56<sup>dim</sup> cells following antibody treatment is calculated relatively to the condition with low dose rhIL-15 and 4 h SKOV-3 stimulation only. Cumulative data are shown as mean+SEM (n = 6) (b) IGROV-1 and OVCAR-3 stimulation for 4 h in the presence of TIGIT and/or DNAM-1 blockade or matching isotype controls. Fold change in CD107a and IFN $\gamma$  expression on CD56<sup>dim</sup> cells following antibody treatment is calculated relatively to the condition with low dose rhIL-15 and 4 h IGROV-1 or OVCAR-3 stimulation only –3 (n = 6 for IGROV-1 and n = 6 for OVCAR). A One-Way repeated measure ANOVA with Bonferroni correction was used for statistical analysis, \*  $p < .05$ , \*\*  $p < .01$  and \*\*\*  $p < .001$ .

bearing NSG mice were infused intraperitoneally with healthy donor NK cells and treated with TIGIT blockade or isotype control twice weekly [Figure 5a](#). rhIL-15 support was given during the 4 weeks in which we acquired tumor load weekly by BLI. NK cell treated mice showed significantly less tumor load compared to no treatment ( $P < .05$ , [Figure 5b](#)). Importantly, NK cell treatment combined with TIGIT blockade resulted in a stronger reduction in tumor load compared to no treatment ( $P < .001$ ). The number of NK cells harvested

at day 33 was similar for both groups [Figure 5c](#). In addition, we performed a degranulation assay on NK cells harvested from each mouse and found that NK cells from mice that had been treated with TIGIT blockade had a significant higher capacity to degranulate and secreted more IFN $\gamma$  compared to mice that received the isotype control [Figure 5d](#). When NK cells from isotype control treated mice were re-stimulated with SKOV-3, subsequent *ex vivo* TIGIT blockade strongly enhanced their CD107a and IFN $\gamma$  levels [Figure 5e](#). DNAM-1 blockade and

**Table 2.** Ovarian cancer (primary) cell line characteristics.

Cell line	CD112 Expression ( $\Delta$ MFI $\pm$ SD)	CD155 Expression ( $\Delta$ MFI $\pm$ SD)
SKOV-3	49.7 ( $\pm$ 8.0)	1040 ( $\pm$ 197)
IGROV-1	31.3 ( $\pm$ 15.5)	1050 ( $\pm$ 350)
OVCAR-3	24.7 ( $\pm$ 15.3)	783 ( $\pm$ 215)
ASC009	22.7 ( $\pm$ 4.9)	1567 ( $\pm$ 116)

CD112 and CD155 expression of ovarian cancer cell lines. SKOV-3, OVCAR-3, IGROV-1 and ASC009 were all acquired on three different time points. Data shown is the average  $\Delta$ MFI with standard deviation.

DNAM-1/TIGIT co-blockade, resulted in a similar reduced degranulation capacity as we observed in our *in vitro* model.

Finally, we investigated TIGIT blockade in ascites-derived NK cells. For this, ascites samples were selected that were collected at diagnosis or first surgery of patients with stage III or IV high-grade serous papillary OC. Patient-derived CD56 positive NK cells were isolated and cultured overnight with low dose (1 nM) rhIL-15 and stimulated with K562 or OC target cells for 4 h. Though heterogeneous, similar degranulation and IFN $\gamma$  responses against K562 were observed overall for ascites-derived and healthy donor CD56<sup>dim</sup> NK cells [figure 5f](#). In contrast, ascites-derived NK cells from several OC patients showed impaired responsiveness to SKOV-3 as compared to healthy donors [Figure 5g](#).

Based on the SKOV-3 degranulation response, patients were grouped in responders ( $\geq$ 10% CD107a<sup>+</sup> CD56<sup>dim</sup> cells) and non-responders (<10% CD107a<sup>+</sup> CD56<sup>dim</sup> cells; [Figure 5g](#) and [Table 1](#)). Next, we compared the response against K562 for both non-responders versus responders. Also here we noticed that CD56<sup>dim</sup> NK cells from non-responders exhibited impaired tumor responsiveness, indicating a more general impairment of the NK cells in these particular patients (Supplemental fig S7A and B). Notably, TIGIT blockade was unable to rescue the NK functionality in these non-responders [Figure 5h](#). Most importantly, TIGIT blockade of CD56<sup>dim</sup> NK cells in responders resulted in significantly enhanced degranulation and IFN $\gamma$  production activity [Figure 5h](#). Simultaneous blockade of TIGIT and DNAM-1 reversed this effect, and again inhibited the degranulation and IFN $\gamma$  production by ascites-derived NK cells. This indicates that also in this setting DNAM-1 triggering is more dominant in NK-mediated targeting of OC tumor cells. Altogether, our data demonstrate that TIGIT blockade boosts functional responsiveness of CD56<sup>dim</sup> NK cells in patients with baseline reactivity against OC tumor cells.

## Discussion

NK cells are regulated via activating and inhibitory receptors, and the net balance of these signals determines whether an NK cell will tolerate or kill a target cell.<sup>43,44</sup> Due to this nature, NK cells have the ability to recognize and destruct tumor cells with increased expression of stress-induced activating ligands and a lack of inhibitory signals. Interestingly, many studies have demonstrated that OC cells are susceptible to killing by activated NK cells,<sup>7-9</sup> hinting that NK cell-based immunotherapy could be an attractive adjuvant treatment for OC patients. However, NK cell antitumor immunity in OC patients can be attenuated by immunosuppressive cells and cytokines within the tumor microenvironment.<sup>13-16</sup> Here, we investigated the role of the DNAM-1/TIGIT/CD96 axis on NK cells in the context of OC. We found that peritoneal NK cells of OC patients consist of different CD56<sup>dim</sup> subpopulations with reduced

DNAM-1 and high TIGIT and CD96 expression, which to a lesser extent can also be found for benign patient peritoneal fluid-derived NK cells. This shift to a more inhibitory phenotype could also be induced *in vitro* by co-culturing healthy donor NK cells with OC tumor spheroids and *in vivo* upon infusion into SKOV-3 OC bearing NSG mice. Other important NK cell receptors such as PD-1, NKG2a, and OX-40 were not affected by interaction with OC cells and spheroids. Interestingly, we were able to counteract DNAM-1 downregulation by adding rhIL-15 to the NK cell-tumor co-cultures, which resulted in a dose-response increase of DNAM-1, TIGIT, and CD96.

The 5 subsets with different DNAM-1/TIGIT/CD96 expression patterns detected in benign and malignant ascites can be induced by a number of factors. First, a study after hematopoietic stem cell transplantation showed that cryopreserved peripheral blood-derived NK cells show a population of CD56<sup>dim</sup>CD16<sup>neg</sup> NK cells that decreases after time which was not observed with fresh cells.<sup>45</sup> However, they could replicate this finding using fresh cells that were stored at room temperature for 24 h indicating a relationship between NK cell viability and this CD56<sup>dim</sup>CD16<sup>neg</sup> population. Other studies have shown that TGF- $\beta$  is able to convert a subset of CD56<sup>dim/bright</sup>CD16<sup>high</sup> NK cells to a CD56<sup>dim/bright</sup>CD16<sup>low/neg</sup> phenotype.<sup>46,47</sup> Additionally, TGF- $\beta$  has been shown to downregulate DNAM-1 and increase CD96 expression on NK cells which is in agreement with our observations.<sup>46,48-50</sup> Since TGF- $\beta$  is known to be present in ascites of OC patients this cytokine may play a role in the altered phenotype of the detected subsets. However, benign patients where the levels of TGF- $\beta$  may be lower also showed a high frequency of CD56<sup>dim</sup>CD16<sup>neg</sup> NK cells. Additionally, CD96 levels on peritoneal NK cells of benign patients appear similar to healthy donor peripheral blood NK cells. Therefore, other factors, such as NK cell activation status, NK cell viability, cytokine stimulation, and tumor cell interaction may be involved to the observed phenotypical alterations in peritoneal NK cells.

In order to functionally boost NK cell reactivity against OC cells, we tested TIGIT blockade. First, in healthy donors, we found that TIGIT blockade enhanced degranulation and IFN $\gamma$  production of healthy donor CD56<sup>dim</sup> NK cells in response to OC tumor cells, especially when DNAM-1/CD155 interactions were in place. In our models, CD96 blockade did not improve nor hamper NK cell functionality, though we cannot exclude the possibility that the used CD96 antibody clone and/or *ex vivo* model-related factors have impacted the results. Most interestingly, we observed that TIGIT blockade boosted functional responsiveness of CD56<sup>dim</sup> NK cells of OC patients with a baseline reactivity against SKOV-3 OC cells.

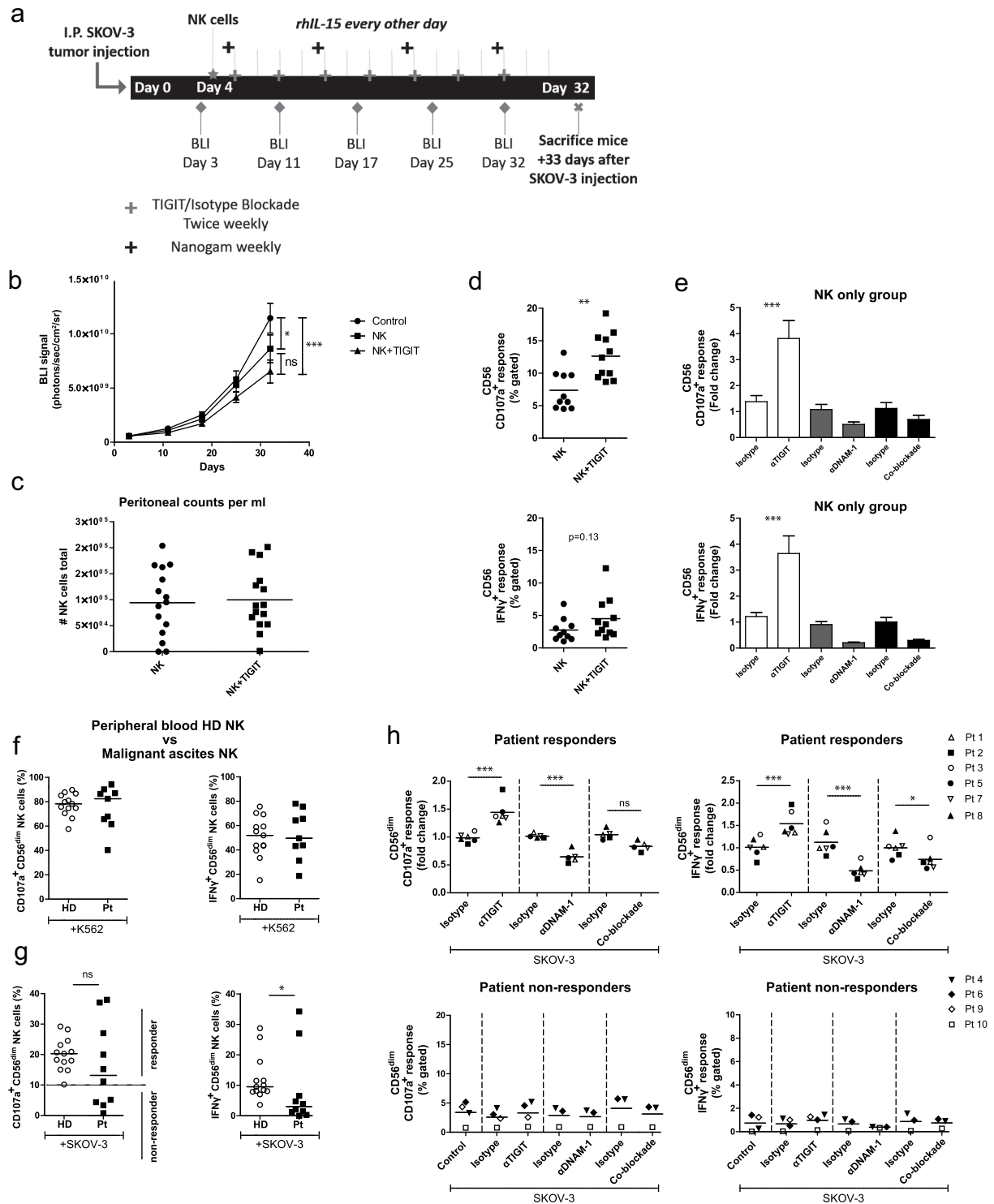


**Figure 5. TIGIT blockade boosts functional responsiveness of CD56<sup>dim</sup> NK cells of OC patients with a baseline reactivity against SKOV-3 cells.** (a) Schematic overview of the mouse experiment. (b) Bioluminescence imaging (BLI) signal of SKOV-3 tumor-bearing mice over time in “control”, “NK” only and “NK+TIGIT” blockade groups (n = 15 per group). (c) Total number of peritoneal NK cells harvested from “NK” only and “NK+TIGIT” blockade groups as measured by flow cytometry (average of bead and volume count cytoflex). (d) Percent CD107a (top graph) and IFN $\gamma$  (bottom graph) from peritoneal NK cells harvested from “NK” only and “NK+TIGIT” groups which were re-stimulated ex-vivo with SKOV-3 for 4 h in the presence of low dose rhIL-15. (e) Percent CD107a (top graph) and IFN $\gamma$  (bottom graph) from peritoneal NK cells harvested from “NK” only group re-stimulated with SKOV-3 in the presence of low dose rhIL-15 in combination with TIGIT, DNAM-1, TIGIT/DNAM-1 co-blockade or corresponding isotype control(s). (f-g) Percentage CD107a<sup>+</sup> and IFN $\gamma$ <sup>+</sup> CD56<sup>dim</sup> NK cells upon overnight treatment with low dose rhIL-15 (1 nM) and subsequent 4 h stimulation with K562 (f) or SKOV-3 (g). Based on a cutoff of 10% CD107a expression on CD56<sup>dim</sup> NK cells co-cultured with SKOV-3 and rhIL-15 (without additional treatment) patients were subdivided in responder ( $\geq 10\%$ ) and non-responder (<10%) cohorts. Cumulative data of healthy donors (HD; n = 10) and ovarian cancer patients (Pt; n = 9) are shown with median. The Mann-Whitney test was used for statistical analysis, \* p < .05. (h) CD56<sup>dim</sup> NK cells positive for CD107a and IFN $\gamma$  after 4 h stimulation with SKOV-3 target cells, low dose rhIL-15 (1 nM), and TIGIT and/or DNAM-1 blockade or matching isotype controls. Cumulative data shown for SKOV-3 responders only (lines indicate mean, n = 6). A One-Way ANOVA with Bonferroni correction was used for statistical analysis, \* p < .05 and \*\*\* p < .001.



Inhibitory phenotypes on NK cells, or on other cell types, are commonly described in the context of cancer as for example melanoma patients have an increased proportion of CD56<sup>dim</sup> CD16<sup>neg</sup> NK cells in tumor biopsies and their prevalence negatively correlated with lytic ability.<sup>51</sup> Our results suggest that these CD56<sup>dim</sup> CD16<sup>neg</sup> cells have a more inhibitory phenotype compared to CD56<sup>dim</sup> CD16<sup>high</sup> and CD16<sup>low</sup> NK cells as they had the lowest DNAM-1 levels, high TIGIT expression and the highest CD96 expression of the three CD56<sup>dim</sup> subsets in both OC patients and patients with benign conditions. CD96<sup>+</sup> NK cells have recently been described to be functionally exhausted with impaired cytokine production which, together with DNAM-1 downregulation, supports that CD56<sup>dim</sup> CD16<sup>neg</sup> NK cells acquired a more inhibitory phenotype.<sup>50</sup> CD96 was also strongly increased by NK cells in SKOV-3 OC bearing NSG mice indicating that, next to TIGIT, it may be an interesting target for future blocking studies in OC. Loss of CD16 in the CD56<sup>dim</sup> CD16<sup>neg</sup> and CD16<sup>low</sup> populations could be due to protein downregulation or CD16 shedding after degranulation as a result of tumor cell contact since CD16 shedding is known to strongly correlate with increased CD107a expression.<sup>52,53</sup> In turn, DNAM-1 also decreases upon tumor cell contact.<sup>34</sup> Therefore, it is possible that CD56<sup>dim</sup> CD16<sup>high</sup> NK cells may become CD56<sup>dim</sup> CD16<sup>low</sup> and later CD56<sup>dim</sup> CD16<sup>neg</sup> during continuous OC tumor engagement but future studies will have to elucidate this phenomenon in more detail.

In our assays, we used rhIL-15 for NK cell survival and found that TIGIT and DNAM-1 expression was increased by rhIL-15 in a dose-dependent manner which is in accordance with literature.<sup>37,54,55</sup> However, after co-incubation of healthy donor NK cells with OC tumor cell spheroids, DNAM-1 expression was strongly reduced and levels were comparably low as ascites-derived NK cells of OC patients. This is in line with our previous results and other studies showing a reduced expression of DNAM-1 on NK cells in OC patients.<sup>34,35</sup> We validated these findings in an *in vivo* model and found that DNAM-1 expression on adoptively transferred NK cells was reduced in SKOV-3 OC bearing mice compared to mice without tumor. In contrast, TIGIT was strongly upregulated in all mice due to rhIL-15 administration to boost NK cell persistence, which is in accordance with our *in vitro* data where we also found increased TIGIT levels upon rhIL-15 stimulation. Carlsten *et al.* showed that CD155 expression specifically reduces DNAM-1 on NK cells by demonstrating that a cell line overexpressing CD155 induced a DNAM-1 reduction whereas CD155 negative cells did not. In addition, they showed that CD155 expression on OC tumor cells from patients negatively correlates with NK cell DNAM-1 expression and that coculture of NK cells and OC cell lines results in DNAM-1 downregulation in a contact-dependent manner.<sup>9,34</sup> These data fit with our findings but we did not find a correlation between CD155 expression and DNAM-1 downregulation, as OVCAR-3 which had the lowest CD155 expression, equally downregulated DNAM-1 compared to SKOV-3 and IGROV-1 which had high CD155 expression levels. This suggests that, besides CD155, ligation with other ligands such as CD112 or other factors may also reduce DNAM-1 expression on NK cells. This is supported by a study in AML patients where

blast CD112 expression was negatively correlated with DNAM-1 expression on NK cells.<sup>32</sup>

Our data show for the first time that TIGIT blockade can enhance NK cell responsiveness toward OC. A beneficial effect of TIGIT blockade on NK cells has already been demonstrated in colon cancer and breast cancer.<sup>39,40</sup> We determined that in SKOV-3 tumor-bearing mice TIGIT blockade yielded more active NK cells compared to control NK cells that did not receive TIGIT blockade. Compared to untreated SKOV-3 tumor-bearing mice, the tumor load was more significantly decreased in NK cell and TIGIT blockade treated mice compared to mice that only received NK cells. Similarly, we observed that TIGIT blockade was able to improve degranulation and IFN $\gamma$  production activity of CD56<sup>dim</sup> NK cells from patients with an *in vitro* baseline response toward SKOV-3 tumor cells. This supports that TIGIT blockade in OC could be a potential immunotherapy for patients with high-grade OC who are now faced with limited treatment options. Our cohort of OC patients was too small to find a correlation between clinical parameters and *in vitro* responders versus non-responders, but a subset of patients evidently showed strongly diminished NK cell reactivity toward OC cells (e.g. SKOV-3). However, these non-responders also showed an impaired response toward K562 target cells, which lack MHC-I expression and are thereby highly sensitive to NK cell attack. It would be interesting to determine the *in vitro* SKOV-3 response of OC patients in the ongoing clinical trial with TIGIT blockade (NCT03628677) and verify whether they observe a similar distribution of responders/non-responders and whether this correlates with clinical outcome of TIGIT blockade. Besides validating our findings it would also be intriguing to unravel the mechanisms underlying non-responsiveness of patient-derived NK cells. One possibility is that these NK cells have a strong inhibitory signature and express few activating receptors leading to an inability to respond to OC tumor cells which we currently investigate in a larger cohort. Another explanation could be that factors in ascitic fluid mediated such a strong inhibitory response that tumor exposure could not re-activate these NK cells. Notably, we found that TIGIT blockade alone was not sufficient to rescue these non-responding NK cells of OC patients. To further investigate the interactions within the DNAM-1/TIGIT pathway we performed co-blockade experiments and observed a net inhibition of NK cell function. Therefore, we concluded that DNAM-1 is the dominant receptor within this checkpoint axis in our OC models. To obtain the highest clinical benefit of TIGIT blockade, probably DNAM-1 needs to be concomitantly upregulated. Accordingly, we demonstrated that TIGIT responsiveness was highest in non-tumor bearing mice, which can be attributed to higher DNAM-1 expression, as compared to tumor-bearing mice. The importance of the DNAM-1 receptor in the context of OC is underscored by our previous study where we showed that OC patients with poor OS have lower DNAM-1 expression on ascites NK cells than patients with a better OS.<sup>35</sup>

Overall, our data show that checkpoint molecules TIGIT/DNAM-1 play an important role in NK cell responsiveness against OC, and provides rationale for incorporating TIGIT interference in NK cell-based immunotherapy in

OC patients. We demonstrate that DNAM-1 expression can be upregulated by rhIL-15 suggesting that TIGIT checkpoint blockade efficacy in OC patients may be optimal in combination with rhIL-15-based stimulation. TIGIT blockade is a highly appealing strategy to boost NK cell functionality as multiple ongoing clinical trials (NCT02794571, NCT03119428, NCT03563716, and NCT03628677) currently investigate the safety, tolerability, and efficacy of TIGIT blockade in patients with advanced metastatic cancers. Since NK cell-based transfer strategies have been shown safe without causing toxicity in multiple cancer types, NK cell adoptive transfer in combination with TIGIT blockade and rhIL-15 could be a promising immunotherapeutic approach in OC patients.







## Acknowledgments

We thank Heleen N. Haspels for technical support. Furthermore, we thank the patients and clinicians who provided the primary material for this study. We would also like to thank G. Zaman for providing us with primary cell line ASC009. This work was supported by grants from RIMLS 2016-7.

## Funding

This work was supported by the Radboudumc/RIMLS [2016-7].

## ORCID

Ralph Ja Maas  <http://orcid.org/0000-0002-3185-5226>  
 Janneke S Hoogstad-van Evert  <http://orcid.org/0000-0001-9838-0977>  
 Jolien Mr Van der Meer  <http://orcid.org/0000-0001-9288-1500>  
 Vera Mekers  <http://orcid.org/0000-0001-6989-7619>  
 Somayeh Rezaeifard  <http://orcid.org/0000-0003-3720-3875>  
 Alan J Korman  <http://orcid.org/0000-0002-1142-8542>  
 Paul Kjd de Jonge  <http://orcid.org/0000-0002-1228-5002>  
 Nicolaas Pm Schaap  <http://orcid.org/0000-0001-7696-4752>  
 Joop H Jansen  <http://orcid.org/0000-0001-9459-568X>  
 Willemijn Hobo  <http://orcid.org/0000-0002-8206-8185>  
 Harry Dolstra  <http://orcid.org/0000-0002-3998-687X>

## Declaration of interest

Alan Korman is an employee of Bristol-Myers Squibb. The remaining authors declare no potential conflicts of interest.

## References

- Ahmed N, Stenvers KL. Getting to know ovarian cancer ascites: opportunities for targeted therapy-based translational research. *Front Oncol.* 2013;3:256.
- Siegel RL, Miller KD, Jemal A. Cancer statistics, 2017. *CA Cancer J Clin.* 2017;67(1):7–30. doi:10.3322/caac.21387.
- James FR, Jimenez-Linan M, Alsop J, Mack M, Song H, Brenton JD, Pharoah PDP, Ali HR. Association between tumour infiltrating lymphocytes, histotype and clinical outcome in epithelial ovarian cancer. *BMC Cancer.* 2017;17(1):657. doi:10.1186/s12885-017-3585-x.
- Zhang L, Conejo-Garcia JR, Katsaros D, Gimotty PA, Massobrio M, Regnani G, Makrigiannakis A, Gray H, Schlienger K, Liebman MN, et al. Intratumoral T cells, recurrence, and survival in epithelial ovarian cancer. *N Engl J Med.* 2003;348(3):203–213. doi:10.1056/NEJMoa020177.
- Hwang WT, Adams SF, Tahirovic E, Hagemann IS, Coukos G. Prognostic significance of tumor-infiltrating T cells in ovarian cancer: a meta-analysis. *Gynecol Oncol.* 2012;124(2):192–198. doi:10.1016/j.ygyno.2011.09.039.
- Webb JR, Milne K, Watson P, deLeeuw RJ, Nelson BH. Tumor-infiltrating lymphocytes expressing the tissue resident memory marker CD103 are associated with increased survival in high-grade serous ovarian cancer. *Clin Cancer Res.* 2014;20(2):434–444. doi:10.1158/1078-0432.CCR-13-1877.
- Geller MA, Knorr DA, Hermanson DA, Pribyl L, Bendzick L, Mccullar V, Miller JS, Kaufman DS. Intraperitoneal delivery of human natural killer cells for treatment of ovarian cancer in a mouse xenograft model. *Cytotherapy.* 2013;15(10):1297–1306. doi:10.1016/j.jcyt.2013.05.022.
- Felices M, Chu S, Kodali B, Bendzick L, Ryan C, Lenvik AJ, Boylan KLM, Wong HC, Skubitz APN, Miller JS, et al. IL-15 super-agonist (ALT-803) enhances natural killer (NK) cell function against ovarian cancer. *Gynecol Oncol.* 2017;145(3):453–461. doi:10.1016/j.ygyno.2017.02.028.
- Carlsten M, Björkström NK, Norell H, Bryceson Y, van Hall T, Baumann BC, Hanson M, Schedvins K, Kiessling R, Ljunggren H-G, et al. DNAX accessory molecule-1 mediated recognition of freshly isolated ovarian carcinoma by resting natural killer cells. *Cancer Res.* 2007;67(3):1317–1325. doi:10.1158/0008-5472.CAN-06-2264.
- Geller MA, Cooley S, Judson PL, Ghebre R, Carson LF, Argenta PA, Jonson AL, Panoskaltis-Mortari A, Curtsinger J, McKenna D, Dusenbery K, et al. A phase II study of allogeneic natural killer cell therapy to treat patients with recurrent ovarian and breast cancer. *Cytotherapy.* 2011;13(1):98–107.
- Yang Y, Lim O, Kim TM, Ahn Y-O, Choi H, Chung H, Min B, Her JH, Cho SY, Keam B, et al. Phase I study of random healthy donor-derived allogeneic natural killer cell therapy in patients with malignant lymphoma or advanced solid tumors. *Cancer Immunol Res.* 2016;4(3):215–224. doi:10.1158/2326-6066.CIR-15-0118.
- Hoogstad-van Evert J, Bekkers R, Ottevanger N, Schaap N, Hobo W, Jansen JH, Massuger L, Dolstra H. Intraperitoneal infusion of ex vivo-cultured allogeneic NK cells in recurrent ovarian carcinoma patients (a phase I study). *Medicine (Baltimore).* 2019;98(5):e14290. doi:10.1097/MD.00000000000014290.
- Yigit R, Massuger LFAG, Figdor CG, Torensma R. Ovarian cancer creates a suppressive microenvironment to escape immune elimination. *Gynecol Oncol.* 2010;117(2):366–372. doi:10.1016/j.ygyno.2010.01.019.
- Yigit R, Figdor CG, Zusterzeel PLM, Pots JM, Torensma R, Massuger LFAG. Cytokine analysis as a tool to understand tumour-host interaction in ovarian cancer. *Eur J Cancer.* 2011;47(12):1883–1889. doi:10.1016/j.ejca.2011.03.026.
- Rodriguez GM, Galpin K, McCloskey C, Vanderhyden B. The Tumor Microenvironment of Epithelial Ovarian Cancer and Its Influence on Response to Immunotherapy. *Cancers (Basel).* 2018;10(8):242. doi:10.3390/cancers10080242.
- Giuntoli RL 2nd, Webb TJ, Zoso A, Rogers O, Diaz-Montes TP, Bristow RE, Oelke M. Ovarian cancer-associated ascites demonstrates altered immune environment: implications for antitumor immunity. *Anticancer Res.* 2009;29(8):2875–2884.
- Fogel LA, Yokoyama WM, French AR. Natural killer cells in human autoimmune disorders. *Arthritis Res Ther.* 2013;15(4):216. doi:10.1186/ar4232.
- Mandal A, Viswanathan C. Natural killer cells: in health and disease. *Hematol Oncol Stem Cell Ther.* 2015;8(2):47–55. doi:10.1016/j.hemonc.2014.11.006.
- Baci D, Bosi A, Gallazzi M, Rizzi M, Noonan DM, Poggi A, Bruno A, Mortara L. The ovarian cancer tumor immune microenvironment (TIME) as target for therapy: a focus on innate immunity cells as therapeutic effectors. *Int J Mol Sci.* 2020;21(9):3125. doi:10.3390/ijms21093125.
- Kwon HJ, Kim N, Kim HS. Molecular checkpoints controlling natural killer cell activation and their modulation for cancer immunotherapy. *Exp Mol Med.* 2017;49(3):e311. doi:10.1038/emmm.2017.42.

21. Sakisaka T, Takai Y. Biology and pathology of nectins and nectin-like molecules. *Curr Opin Cell Biol.* 2004;16(5):513–521. doi:10.1016/j.ceb.2004.07.007.
22. Fuchs A, Colonna M. The role of NK cell recognition of nectin and nectin-like proteins in tumor immunosurveillance. *Semin Cancer Biol.* 2006;16(5):359–366. doi:10.1016/j.semcancer.2006.07.002.
23. Cerboni C, Fionda C, Soriani A, Zingoni A, Doria M, Cippitelli M, Santoni A.. The DNA damage response: a common pathway in the regulation of NKG2D and DNAM-1 ligand expression in normal, infected, and cancer cells. *Front Immunol.* 2013;4:508.
24. Smazynski J, Hamilton PT, Thornton S, Milne K, Wouters MCA, Webb JR, Nelson BH. The immune suppressive factors CD155 and PD-L1 show contrasting expression patterns and immune correlates in ovarian and other cancers. *Gynecol Oncol.* 2020;158(1):167–177. doi:10.1016/j.ygyno.2020.04.689.
25. Martinet L, Smyth MJ. Balancing natural killer cell activation through paired receptors. *Nat Rev Immunol.* 2015;15(4):243. doi:10.1038/nri3799.
26. Deuss FA, Gully BS, Rossjohn J, Berry R. Recognition of nectin-2 by the natural killer cell receptor T cell immunoglobulin and ITIM domain (TIGIT). *J Biol Chem.* 2017;292(27):11413–11422. doi:10.1074/jbc.M117.786483.
27. Wang H, Qi J, Zhang S, Li Y, Tan S, Gao GF. Binding mode of the side-by-side two-IgV molecule CD226/DNAM-1 to its ligand CD155/Necl-5. *Proc Natl Acad Sci U S A.* 2019;116(3):988–996. doi:10.1073/pnas.1815716116.
28. Shibuya A, Campbell D, Hannum C, Yssel H, Franz-Bacon K, McClanahan T, Kitamura T, Nicholl J, Sutherland GR, Lanier LL, et al. DNAM-1, a novel adhesion molecule involved in the cytolytic function of T lymphocytes. *Immunity.* 1996;4(6):573–581. doi:10.1016/S1074-7613(00)70060-4.
29. Stanitsky N, Simic H, Arapovic J, Toporik A, Levy O, Novik A, Levine Z, Beiman M, Dassa L, Achdout H, et al. The interaction of TIGIT with PVR and PVRL2 inhibits human NK cell cytotoxicity. *Proc Natl Acad Sci U S A.* 2009;106(42):17858–17863.
30. Liu S, Zhang H, Li M, Hu D, Li C, Ge B, Jin B, Fan Z. Recruitment of Grb2 and SHIP1 by the ITT-like motif of TIGIT suppresses granule polarization and cytotoxicity of NK cells. *Cell Death Differ.* 2013;20(3):456–464. doi:10.1038/cdd.2012.141.
31. Sanchez-Correa B, Valhondo I, Hassouneh F, Lopez-Sejas N, Pera A, Bergua JM, Arcos MJ, Bañas H, Casas-Avilés I, Durán E, et al. DNAM-1 and the TIGIT/PVRIG/TACTILE Axis: novel immune checkpoints for natural killer cell-based cancer immunotherapy. *Cancers (Basel).* 2019;11(6):877. doi:10.3390/cancers11060877.
32. Sanchez-Correa B, Gayoso I, Bergua JM, Casado JG, Morgado S, Solana R, Tarazona R. Decreased expression of DNAM-1 on NK cells from acute myeloid leukemia patients. *Immunol Cell Biol.* 2012;90(1):109–115. doi:10.1038/icb.2011.15.
33. Zhang Z, Wu N, Lu Y, Davidson D, Colonna M, Veillette A. DNAM-1 controls NK cell activation via an ITT-like motif. *J Exp Med.* 2015;212(12):2165–2182. doi:10.1084/jem.20150792.
34. Carlsten M, Norell H, Bryceson YT, Poschke I, Schedvins K, Ljunggren HG, Kiessling R, Malmberg KJ, et al. Primary human tumor cells expressing CD155 impair tumor targeting by down-regulating DNAM-1 on NK cells. *J Immunol.* 2009;183(8):4921–4930. doi:10.4049/jimmunol.0901226.
35. Hoogstad-van Evert JS, Maas RJ, Van Der Meer J, Cany J, Van Der Steen S, Jansen JH, Miller JS, Bekkers R, Hobo W, Massuger L, Dolstra H, et al. Peritoneal NK cells are responsive to IL-15 and percentages are correlated with outcome in advanced ovarian cancer patients. *Oncotarget.* 2018;9(78):34810–34820. doi:10.18632/oncotarget.26199.
36. Hattori N, Kawaguchi Y, Sasaki Y, Shimada S, Murai S, Abe M, Baba Y, Watanuki M, Fujiwara S, Arai N, et al. Monitoring TIGIT/DNAM-1 and PVR/PVRL2 immune checkpoint expression levels in allogeneic stem cell transplantation for acute myeloid leukemia. *Biol Blood Marrow Transplant.* 2019;25(5):861–867. doi:10.1016/j.bbmt.2019.01.013.
37. Sarhan D, Cichocki F, Zhang B, Yingst A, Spellman SR, Colley S, Verneris MR, Blazar BR, Miller JS, et al. Adaptive NK cells with low TIGIT expression are inherently resistant to myeloid-derived suppressor cells. *Cancer Res.* 2016;76(19):5696–5706. doi:10.1158/0008-5472.CAN-16-0839.
38. Wang F, Hou H, Wu S, Tang Q, Liu W, Huang M, Yin B, Huang J, Mao L, Lu Y, Sun Z, et al. TIGIT expression levels on human NK cells correlate with functional heterogeneity among healthy individuals. *Eur J Immunol.* 2015;45(10):2886–2897. doi:10.1002/eji.201545480.
39. Zhang Q, Bi J, Zheng X, Chen Y, Wang H, Wu W, Wang Z, Wu Q, Peng H, Wei H, Sun R, et al. Blockade of the checkpoint receptor TIGIT prevents NK cell exhaustion and elicits potent anti-tumor immunity. *Nat Immunol.* 2018;19(7):723–732. doi:10.1038/s41590-018-0132-0.
40. Xu F, Sunderland A, Zhou Y, Schulick RD, Edil BH, Zhu Y. Blockade of CD112R and TIGIT signaling sensitizes human natural killer cell functions. *Cancer Immunol Immunother.* 2017;66(10):1367–1375. doi:10.1007/s00262-017-2031-x.
41. Giannattasio A, Weil S, Kloess S, Ansari N, Stelzer EHK, Cerwenka A, Steinle A, Koehl U, Koch J. Cytotoxicity and infiltration of human NK cells in in vivo-like tumor spheroids. *BMC Cancer.* 2015;15(1):351. doi:10.1186/s12885-015-1321-y.
42. Friedrich J, Seidel C, Ebner R, Kunz-Schughart LA. Spheroid-based drug screen: considerations and practical approach. *Nat Protoc.* 2009;4(3):309–324. doi:10.1038/nprot.2008.226.
43. Kiessling R, Klein E, Wiggzell H. “Natural” killer cells in the mouse. I. Cytotoxic cells with specificity for mouse Moloney leukemia cells. Specificity and distribution according to genotype. *Eur J Immunol.* 1975;5(2):112–117. doi:10.1002/eji.1830050208.
44. Herberman RB, Nunn ME, Lavrin DH. Natural cytotoxic reactivity of mouse lymphoid cells against syngeneic acid allogeneic tumors. I. Distribution of reactivity and specificity. *Int J Cancer.* 1975;16(2):216–229. doi:10.1002/ijc.2910160204.
45. Lugthart G, van Ostaijen-ten Dam MM, van Tol MJD, Lankester AC, Schilham MW. CD56(dim)CD16<sup>+</sup> NK cell phenotype can be induced by cryopreservation. *Blood.* 2015;125(11):1842–1843. doi:10.1182/blood-2014-11-610311.
46. Xu Y, Sun J, Sheard MA, Tran HC, Wan Z, Liu WY, Asgharzadeh S, Sposto R, Wu HW, Seeger RC, et al. Lenalidomide overcomes suppression of human natural killer cell anti-tumor functions by neuroblastoma microenvironment-associated IL-6 and TGFβ1. *Cancer Immunol Immunother.* 2013;62(10):1637–1648. doi:10.1007/s00262-013-1466-y.
47. Allan DS, Rybalov B, Awong G, Zúñiga-Pflücker JC, Kopcow HD, Carlyle JR, Strominger JL. TGF-β affects development and differentiation of human natural killer cell subsets. *Eur J Immunol.* 2010;40(8):2289–2295. doi:10.1002/eji.200939910.
48. Tran HC, Wan Z, Sheard MA, Sun J, Jackson JR, Malvar J, Xu Y, Wang L, Sposto R, Kim ES, et al. TGFβR1 blockade with galunisertib (LY2157299) enhances anti-neuroblastoma activity of the anti-GD2 antibody dinutuximab (ch14.18) with natural killer cells. *Clin Cancer Res.* 2017;23(3):804–813. doi:10.1158/1078-0432.CCR-16-1743.
49. Wilson EB, El-Jawhari JJ, Neilson AL, Hall GD, Melcher AA, Meade JL, Cook GP. Human tumour immune evasion via TGF-β blocks NK cell activation but not survival allowing therapeutic restoration of anti-tumour activity. *PLoS One.* 2011;6(9):e22842. doi:10.1371/journal.pone.0022842.
50. Sun H, Huang Q, Huang M, Wen H, Lin R, Zheng M, Qu K, Li K, Wei H, Xiao W, et al. Human CD96 correlates to natural killer cell exhaustion and predicts the prognosis of human hepatocellular carcinoma. *Hepatology.* 2019;70(1):168–183. doi:10.1002/hep.30347.
51. Vujanovic L, Chuckran C, Lin Y, Ding F, Sander CA, Santos PM, Lohr J, Mashadi-Hosseini A, Warren S, White A, et al. CD56(dim)CD16(-) natural killer cell profiling in melanoma patients receiving a cancer vaccine and interferon-alpha. *Front Immunol.* 2019;10:14. doi:10.3389/fimmu.2019.00014.
52. Romeo R, Foley B, Lenvik T, Wang Y, Zhang B, Ankario D, Luo X, Cooley S, Verneris M, Walcheck B, Miller J, et al. NK cell CD16 surface expression and function is regulated by a disintegrin and metalloprotease-17 (ADAM17). *Blood.* 2013;121(18):3599–3608. doi:10.1182/blood-2012-04-425397.

53. Grzywacz B, Kataria N, Verneris MR. CD56dimCD16+ NK cells downregulate CD16 following target cell induced activation of matrix metalloproteinases. *Leukemia*. 2007;21(2):356–359. doi:10.1038/sj.leu.2404499.
54. Szczepanski MJ, Szajnik M, Welsh A, Foon KA, Whiteside TL, Boyiadzis M. Interleukin-15 enhances natural killer cell cytotoxicity in patients with acute myeloid leukemia by upregulating the activating NK cell receptors. *Cancer Immunol Immunother*. 2010;59(1):73–79. doi:10.1007/s00262-009-0724-5.
55. de Rham C, Ferrari-Lacraz S, Jendly S, Schneiter G, Dayer J-M, Villard J. The proinflammatory cytokines IL-2, IL-15 and IL-21 modulate the repertoire of mature human natural killer cell receptors. *Arthritis Res Ther*. 2007;9(6):R125. doi:10.1186/ar2336.